

Thesis for the Degree of Master of Science

Development of a correcting  
method of wind velocity simulated  
by the WRF model in urban areas



by

Ho-Jin Yang

Department of Environmental Atmospheric Sciences

The Graduate school

Pukyong National University

February 2013

Development of a correcting method of  
wind velocity simulated by the WRF  
model in urban areas

도시지역에서 WRF 모델 모의 풍속 보정 방안 개발

Advisor: Prof. Jae-Jin Kim

by  
Ho-Jin Yang

A thesis submitted in partial fulfillment of the requirements  
for the degree of

Master of Science

in Department of Environmental Atmospheric Sciences, the  
Graduate School  
Pukyong National University

February 2013

Development of a correcting method of wind velocity  
simulated by the WRF model in urban areas

A dissertation

by

Ho-Jin Yang

Approved by:

(Chairman)

Hyeong-Bin Cheong

(Member)

Byoung-Hyuk Kwon

(Member)

Jae-In Kim

February 22, 2013

# Contents

List of Figures .....	ii
List of Tables .....	v
Abstract .....	vi
1. Introduction .....	1
2. Methodology .....	4
2.1. Experimental set up .....	4
2.1.1. WRF model .....	4
2.1.2. CFD model .....	8
2.2. Target areas .....	11
2.3. Surface boundary input data .....	13
3. Results and discussions .....	17
3.1. WRF simulation .....	17
3.2. CFD simulation .....	19
3.3. Build volume fraction .....	21
3.4. Multiple regression analysis .....	27
3.5. Validation .....	30
4. Summary and conclusions .....	34
5. Reference .....	36

# List of Figures

Fig. 1. Model domain in WRF simulation. ....	7
Fig. 2. Grid system of CFD model. ....	10
Fig. 3. Aerial photograph around (a) Gangnam AWS, (b) Yangcheon AWS, (c) Pyeongtaek AWS. ....	12
Fig. 4. Aerial photograph around (a) Gangnam AWS, (b) Yangcheon AWS, (c) Pyeongtaek AWS. ....	14
Fig. 5. Generation of surface building input data and topography input data. ....	15
Fig. 6. Surface input data of (a) Gangnam, (b) Yangcheon, (c) Pyeongtaek. ....	16
Fig. 7. Comparison of simulated wind speed of WRF model and observed wind speed at (a) Gangnam, (b) Yangcheon, and (c) Pyeongtaek. ....	18
Fig. 8. Simulated wind speed of CFD model against the inflow and inflow at (a) Gangnam AWS, (b) Yangcheon AWS, (c) Pyeongtaek AWS. ....	21
Fig. 9. Algorithm of building volume fraction calculation. ....	23

Fig. 10. Correlation Analysis of wind speed and building volume fraction at Gangnam. ....	24
Fig. 11. Correlation Analysis of wind speed and building volume fraction at Yangcheon. ....	25
Fig. 12. Correlation Analysis of wind speed and building volume fraction at Pyeongtaek. ....	26
Fig. 13. (a) simulated wind direction of WRF model and (b) comparison of simulated wind speed of WRF model, observed wind speed, and corrected wind speed at Gangnam. ....	31
Fig. 14. (a) simulated wind direction of WRF model and (b) comparison of simulated wind speed of WRF model, observed wind speed, and corrected wind speed at Yangcheon. ....	32
Fig. 15. (a) simulated wind direction of WRF model and (b) comparison of simulated wind speed of WRF model, observed wind speed, and corrected wind speed at Pyungtaek. ....	33

## List of Tables

Table 1. Experimental description of WRF model. ....	6
Table 2. The building volume fraction with consideration for R and $\theta$ . ....	23
Table 3. Correction coefficients of 16 wind directions at Target areas. ...	29



# 도시지역에서 WRF 모델 모의 풍속 보정 방안 개발

양 호 진

부 경 대 학 교 대 학 원 환 경 대 기 과 학 과

요 약

본 연구에서는 도시 지역 내 구조물의 영향을 중규모 모델 WRF 모의 풍속에 반영 할 수 있는 방안으로 건물 부피비를 이용하여 보정 계수를 개발 하였다. 대상지역으로 도시지역의 특성을 잘 반영할 수 있는 지역의 관측소 주변지역을 선택하여 WRF 모의 풍속과 AWS 관측 풍속을 비교하였다. 비교 결과, WRF 모의 풍속이 AWS 관측 풍속과 비교하여 다소 과대모의 되는 경향을 보였다. 도시지역의 구조물이 풍속 변화에 미치는 영향을 확인하기 위하여, GIS자료를 이용하여 대상지역의 현실적인 상세 지표 경계 입력 자료를 구축하고 16방위의 유입류를 고려한 CFD 수치모의를 실시하였다. CFD 수치모의 결과, 주변 건물에 의한 영향으로 유입류에 비해 관측지점에서의 풍속이 감소됨을 확인 하였다. 관측 지점 주변의 건물들이 풍속 변화에 어떤 영향을 미치는지 조사하기 위하여 방위각과 반경을 고려한 16방위별 풍상측 건물 부피비 산정 알고리즘을 개발하였다. 개발된 건물 부피비 산정 알고리즘을 사용하여 대상지역의 16방위별 건물 부피를 산정하였다. 산정된 대상지역의 16방위별 건물 부피비와 풍속 변화와의 상관관계를 조사한 결과, 대상지역에서 음의 상관관계가 나타났으며, 풍상측 건물 부피가 증가할수록 풍속이 감소되고 있음을 확인하였다. 건물의 영향을 WRF 모의 풍속에 반영시키기 위하여 CFD 수치모의 결과와 건물 부피비를 이용하여 다중회귀분석을 통한 방위각과 반경별 건물의 영향을 반영한 보정 계수를 산출하였다. 대상 지역별로 산출된 보정계수를 이용하여 WRF 모의 풍속을 보정한 결과, 실제 관측 풍속에 가깝게 보정됨을 확인할 수 있었다.

# 1. Introduction

Over the past several decades, increasing urbanization has induced population growth and increased industrial facilities in urban areas. 52.1% of the world's population and 83.2 % of the Republic of Korea's population live in urban areas(UN, 2012). The phenomenon of air pollution due to human activity is concentrated in these urban areas. In densely populated urban areas, investigation of air pollution is very important because prolonged exposure to pollutants can cause severe damage to human body(choi et. al., 2002). On a local scale, meteorological factors are very important on the flow and dispersion of these pollutants. Therefore, forecasting meteorological factors is necessary. Observational data from weather observation stations is ideal for investigation of meteorological factors(Lee et al, 2003).

Weather observational data provides realistic data. However, Observational data has spatial limitations and it is impossible to predict the future. To overcome these kinds of problems, the mesoscale meteorological models are used widely to predict factors without spatial constraints. However, mesoscale meteorological models cannot simulate meteorological factors that reflect the impact of surface obstacles in urban areas (Otte, 2003).

In urban area, buildings are a very important forcing on flow

and dispersion. For this reason, there is a big disconnect between observational data and simulated meteorological factors because urban structures cause obstruction effects such as friction effects and separation of flow that distort results. To improve the mesoscale model simulation of meteorological fields in urban areas, investigation about the effects of buildings on the meteorological fields is necessary.

Much research has been carried out to understand the air flow and dispersion in urban areas. Experimental methods such as field, wind tunnel and water tank experiments are used to understand the effects of obstacles on flow and dispersion(DePaul and Sheih, 1985, 1986; Nakamura and Oke, 1988; Rotach, 1995; Meroney et al., 1996; Baik et al., 2000; Brown et al., 2000; Uehara et al., 2000; Liu et al., 2003; Kim and Baik, 2005). Experimental methods provide realistic flow characteristics by reproducing real conditions. However, it is hard to repeat experiments which is applied to variety of conditions because it need expensive nature.

To overcome these kinds of problem, numerical experiments are commonly used to apply various physical conditions at a low cost.(Lee and Park, 1994; Sini et al., 1996; Baik and Kim, 1999; Kim and Baik, 1999, 2001; Liu and Barth, 2002; Baik et al., 2003; Cheng and Hu, 2005).

Most meteorological models have difficulties in factoring for the effects that building have on data due to their limitation in coordinate

systems and resolution. However, Computational Fluid Dynamics(CFD) models which are commonly used for numerical experiments can take into account these building effects and provide accurate and detailed flow and dispersion(Kim and Baik, 2005; Lee and Kim, 2011; Baik et al., 2003).

In order to consider building effects on urban areas, detailed topography data is needed. Detailed topography data can be obtained by Geographical Information System(GIS). Many studies have recently used GIS data to simulate realistic flow and dispersion in urban areas(Lee and Kim, 2011; Baik et al., 2009).

The aim of this study is to investigate the effects of buildings on urban areas and develop a correction coefficient for simulated wind speeds by mesoscale model. In this study, CFD model simulates the flow in urban areas using surface boundary input data which is constructed using GIS data. The effects of buildings on wind speed are investigated by using numerical simulation results. And Correction coefficient is developed using calculated building fraction from GIS data. The correction coefficient is applied to the simulated wind speed by mesoscale model. The result of application is verified and analyzed.

## 2. Methodology

### 2.1. Experimental set up

#### 2.1.1. WRF model

As a mesoscale model, Weather Research and Forecasting (WRF) model v3.2 which is used widely for prediction of a mesoscale weather phenomena is used in this study.

Table 1 shows an experimental set up of the WRF model and several physical processes. The time integral of the WRF model uses the Runge-Kutta 3rd order. Microphysics is represented with a WSM 6-class graupel scheme (Hong and Lim, 2006). The radiative processes are presented with the RRTM (Rapid Radiative Transfer Model) scheme (Mlawer et al., 1997) for long wave radiation and Dudhia scheme for a short wave radiation. Surface layer physics processes are presented with the Monin-Obukhov (Janjic) scheme, and the Unified Noah Land-Surface Model (Mitchell, 2005) is used for land surface physics. Planetary boundary layer processes are presented with the Mellor-Yamada Janjic TKE scheme (Janjic, 1994) and the Kain-Fritsch Eta scheme (Kain and Fritsch, 1993) is used for cloud

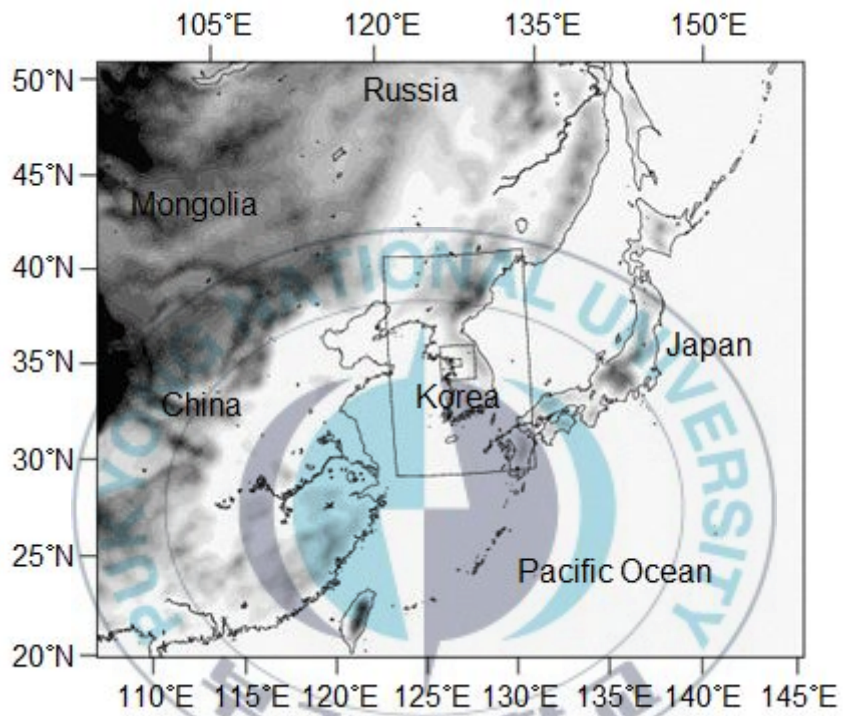
physics processes.

Fig 1 shows the computational domain used in WRF model. WRF domain consist of four one-way nested computational domains which are considered with horizontal grid intervals of 27, 9, 3, 1 km. The horizontal grid dimension is respectively  $179 \times 143$ ,  $93 \times 147$ ,  $69 \times 69$ ,  $60 \times 48$ . There are 27 vertical layers in total. NCEP (National Centers for Environmental Prediction) FNL(Final) analysis data is used as initial and boundary conditions in the WRF simulation.



**Table 1.** Experimental description of WRF model.

	Domain 1	Domain 2	Domain 3	Domain 4
Horizontal grid dimension	179 × 143	93 × 147	69 × 69	60 × 49
Vertical layers	27 (eta level)			
Horizontal grid size (km)	27	9	3	1
Microphysics	WSM 6-class graupel scheme			
Longwave radiation	Rapid Radiative Transfer Model (RRTM)			
Shortwave radiation	Dudhia scheme			
Surface layer	Monin–Obukhov (Janjic) scheme			
Boundary layer	Mellor–Yamada–JanjicTKE scheme			
Cumulus option	Kain–Fritsch (new Eta) scheme		none	
Initial/boundary conditions	NCEP final analysis data (6-h intervals, 1° × 1° resolution)			



**Fig. 1.** Model domain in WRF simulation.

## 2.1.2. CFD model

The CFD model used in this study is the same as the one used by Kim (2007). This model is based on the Reynolds-averaged Navier-Stokes equations (RANS). The CFD model also employs a three-dimensional, non-hydrostatic, non-rotating, incompressible airflow system that negates the coriolis effect. Renormalization group (RNG)  $k$ - $\epsilon$  turbulence model is used for turbulence parametrization (Yakhot et al., 1992). The governing equations are numerically solved on a staggered grid system using a finite volume method and Semi-Implicit Method for Pressure-Linked Equation algorithm (Patankar, 1980). And wall boundary conditions are implemented (Versteeg and Malalasekera, 1995).

Inflow boundary condition, turbulent kinetic energy and its dissipation rate are specified as

$$U(z) = \frac{U_*}{\kappa} \ln\left(\frac{z}{z_0}\right) \cos\theta \quad (1)$$

$$V(z) = \frac{U_*}{\kappa} \ln\left(\frac{z}{z_0}\right) \sin\theta \quad (2)$$

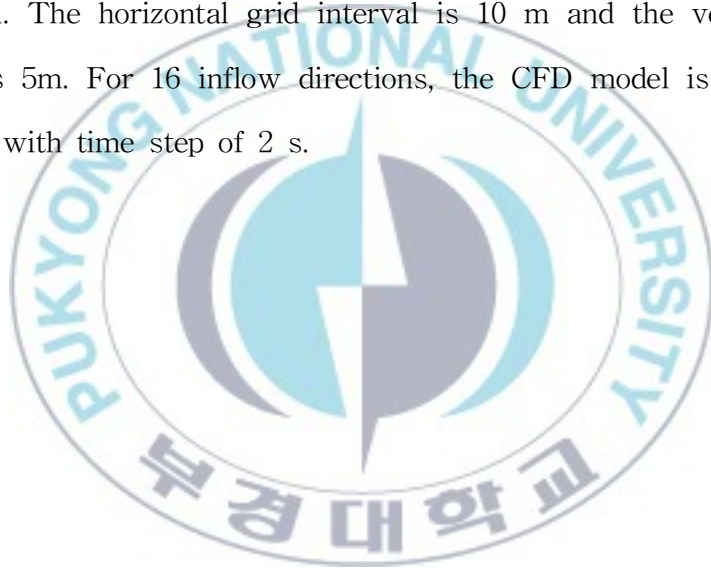
$$W(z) = 0 \quad (3)$$

$$k(z) = \frac{1}{C_\mu^{1/2}} U_*^2 \left(1 - \frac{z}{\delta}\right)^2 \quad (4)$$

$$\varepsilon(z) = \frac{C_{\mu}^{3/4} k^{3/2}}{\kappa z} \quad (5)$$

Here,  $\theta$ ,  $U_*$ ,  $z_0$ ,  $\delta$  and  $\kappa$  are the wind direction, friction velocity, roughness length (= 0.05 m), boundary layer depth (= 1000 m) and von Karman constant (= 0.4) respectively.

Fig 2 shows numerical domain used in CFD model. Domain size is 2000 m in x-direction, 2000 m in y-direction, and 800 m in z-direction. The horizontal grid interval is 10 m and the vertical grid interval is 5m. For 16 inflow directions, the CFD model is integrated for 3600s with time step of 2 s.



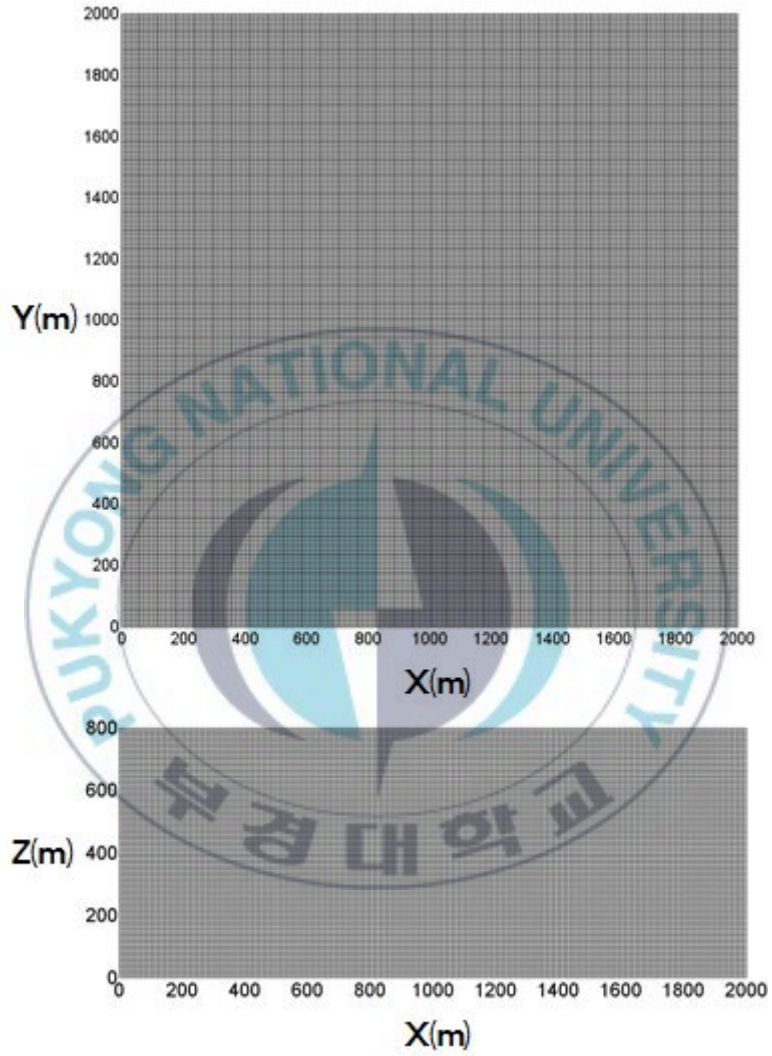


Fig. 2. Grid system of CFD model.

## 2.2. Target areas

In this study, a 2000 m × 2000 m area with an observation station in Gangnam, Yangcheon, Pyeongtaek was set to target areas. The target areas reflect the characteristics of the urban areas very well.

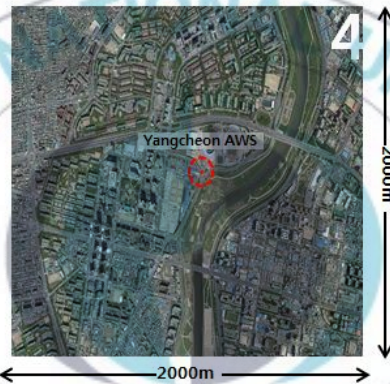
Fig 3 shows aerial photographs of the target areas. The red circle presents the location of AWS observation station. In the Gangnam, more than 20-storey apartment complexes, high-rise buildings, residential and commercial areas are located around the observation station. In Yangcheon, high-rise buildings that include buildings over 50 floor are located around the observation station. Also, a large number of apartment complexes are located around the observation station in Pyeongtaek.

The target areas are enough to reflect the urban effects by building because there are a lot of buildings around the target areas.

(a)



(b)



(c)

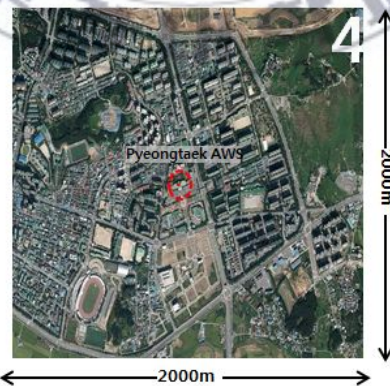


**Fig. 3.** Aerial photograph around (a) Gangnam AWS, (b) Yangcheon AWS, (c) Pyeongtaek AWS.

## 2.3. Surface boundary input data

In order to reflect the realistic effects of urban structures, detailed topography information data from GIS was used as boundary input data for CFD.

Fig 4 shows generation process of building and terrain boundary data from GIS. To make a building boundary input data, the data was extracted from numerical maps in the form of ASCII. But due to the limitations of computing powers, the resolution of building boundary input data is reduced by 10% by the same method used by Lee and Kim (2011). Terrain boundary input data was made by the same process as well. The Surface boundary input data used in numerical model is created by combining building boundary input data and terrain boundary input data

Fig 6 shows surface boundary input data of target areas. The yellow part represent the high-rise buildings that may influence the observation data.

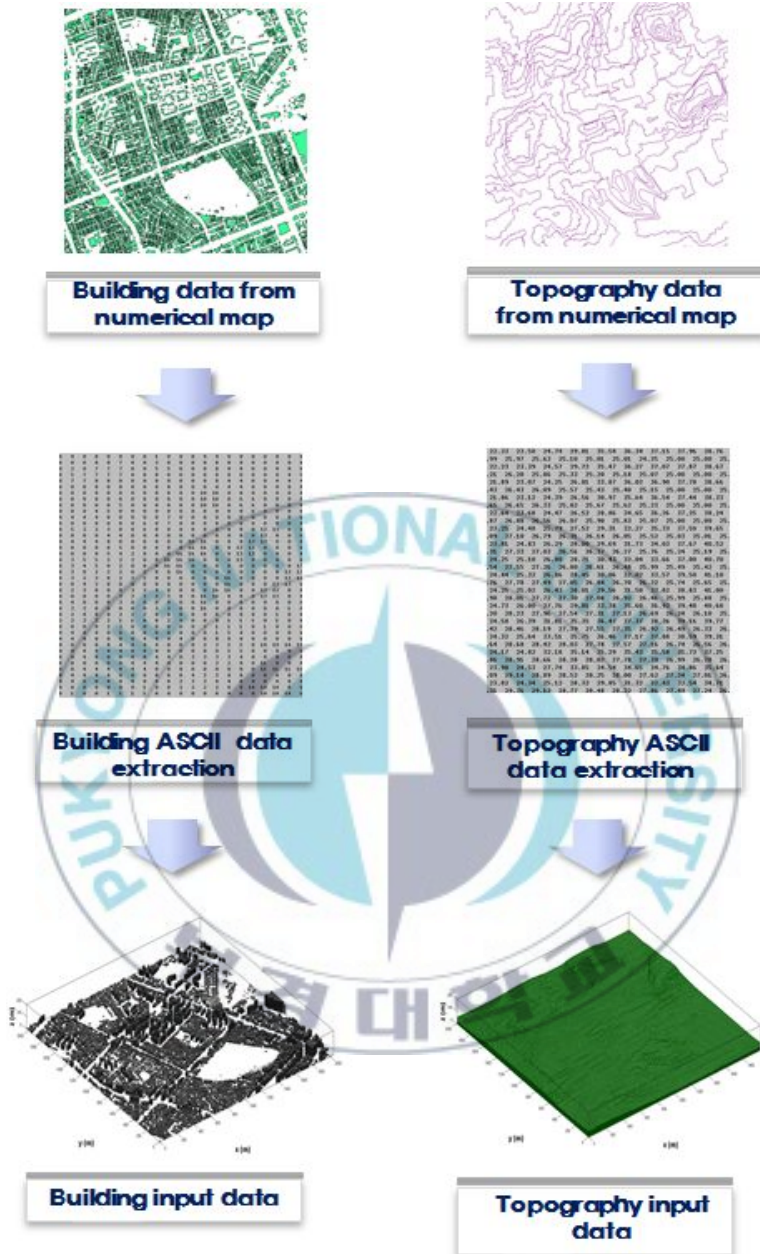
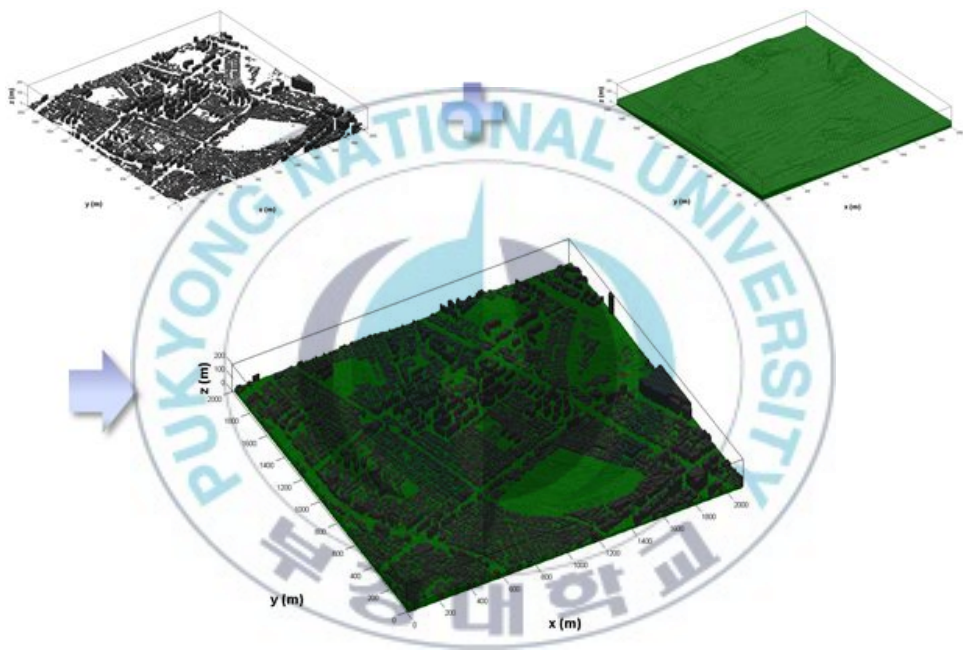
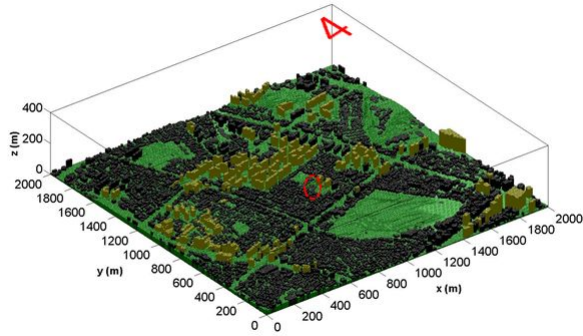


Fig. 4. Generation of surface building input data and topography input data.



**Fig. 5.** Generation of surface input data.

(a)



(b)



(c)

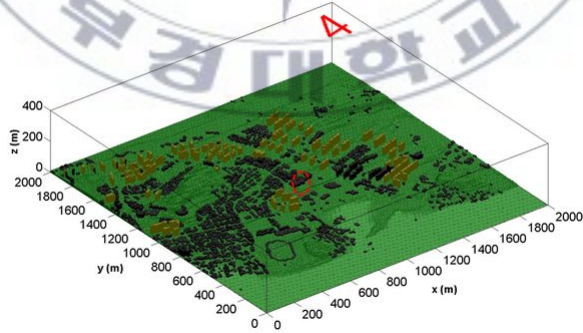


**Fig. 6.** Surface input data of (a) Gangnam, (b) Yangcheon, (c) Pyeongtaek.

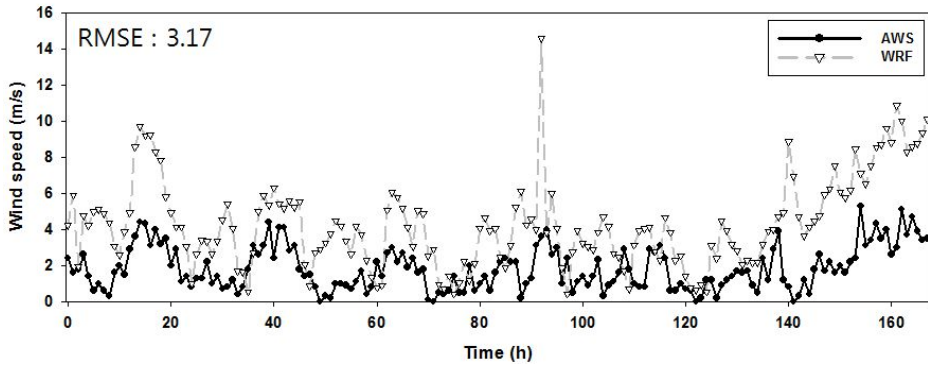
### 3. Results and disscussions

#### 3.1. WRF simulation

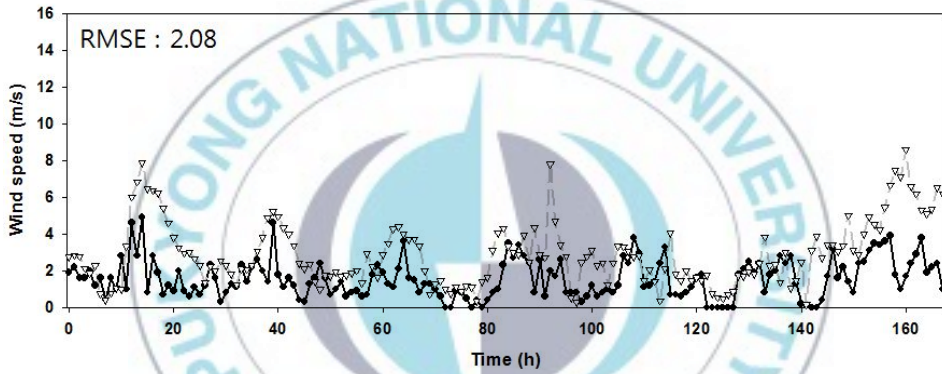
The simulated wind speed by WRF model was compared to the observational wind speed in order to investigate the accuracy of WRF model simulation result in urban areas. The compared period is selected from April 3rd to April 9th in 2008 in order to match with the production year of the GIS data. In all of target areas, the result of the comparison appear to be that the simulated wind speed by WRF model tend to overestimate the effect more than the observational wind speed, as show in Fig. 7.

The relationship between simulated wind speed was quantitatively evaluated with the observed wind speed. The root-mean-square error (RMSE) between the simulated wind speed and observed wind speed in Gangnam, Yangcheon, and Pyeongtaek are 3.17, 2.08, and 2.80  $\text{ms}^{-1}$ , respectively. This confirms that the WRF model does not fully reflect the effects of building on urban areas. Therefore, the effects of building in target areas are investigated by using the CFD model.

(a)



(b)



(c)

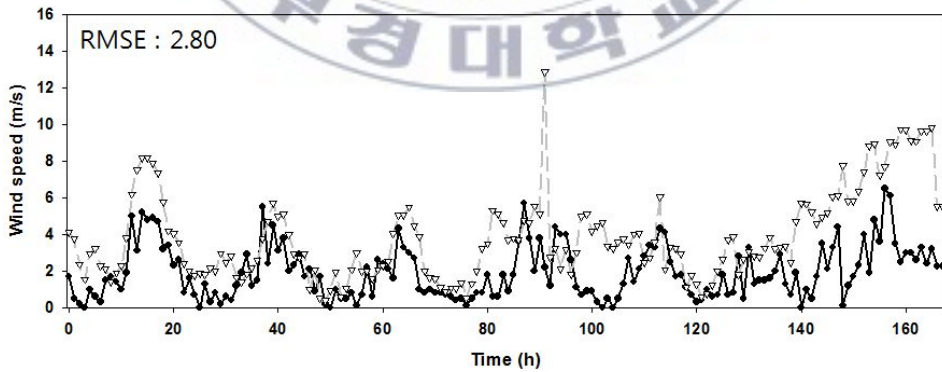


**Fig. 7.** Comparison of simulated wind speed of WRF model and observed wind speed at (a) Gangnam, (b) Yangcheon, and (c) Pyeongtaek.

## 3.2. CFD simulation

In order to investigate the effects of building in target areas, numerical simulation using CFD model was performed. Numerical simulations are carried out for sixteen inflow directions( N, NNE, NE, ENE, E, ESE, SE, SSE, S, SSW, SW, WSW, W, WNW, NW, NNW)

Fig. 8 shows Simulated wind speed of CFD model against the inflow and inflow at Gangnam AWS, Yangcheon AWS, and Pyeongtaek AWS. Here, the blue circle is inflow wind speed and the red points are the simulated wind speed from the CFD model against the inflow of the 16 directions.

In the case of Gangnam, the wind speed was decreased in all of directions. Especially in the northerly and easterly directions. This is due to the large amount of high-rise buildings that are located at the northern and eastern parts of AWS. When the wind is blowing from the south, the wind speed at AWS is close to the inflow wind speed because buildings are non-existent at south of Gangnam AWS.

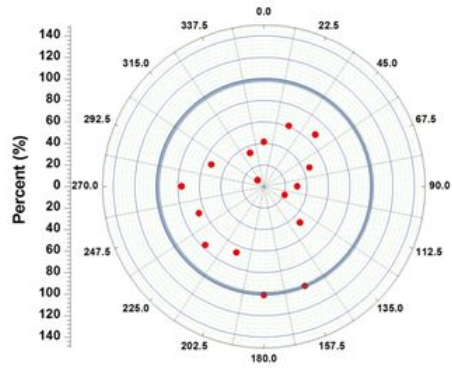
In the case of Yangcheon, the wind speed is decreased except for the wind that blows from the east and south-east which contain very few building. Wind speed is especially deceased in the south-west wind direction because there are many super high-rise buildings there.

In Pyeongtaek, the wind speed is decreased for the wind that blows from the north and north-east which contain apartment complex.

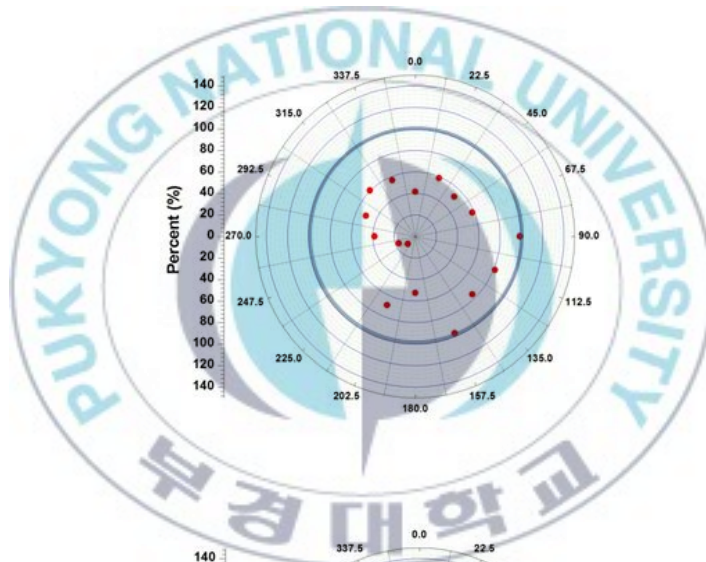
The results of simulating the 16 directions has shown that the buildings on the up-wind side causes the wind decrease against the inflow at observation point.



(a)



(b)



(c)

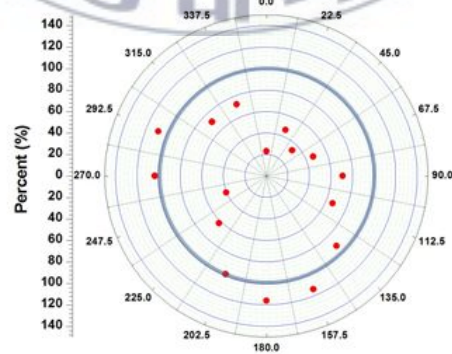


**Fig. 8.** Simulated wind speed of CFD model against the inflow and inflow at (a) Gangnam AWS, (b) Yangcheon AWS, (c) Pyeongtaek AWS.

### 3.3. Building volume fraction

As results of CFD simulation, the buildings on the up-wind side causes the wind decrease against the inflow at observation point.

In order to fully analyze the effects of building on the up-wind side, the building volume fraction, which considers azimuth and radius from the observation point, was evaluated for correlation with change of wind speed at all of the target areas.

Fig. 9 shows Algorithm of building volume fraction calculation. Here,  $\Theta$  is azimuth and  $R$  is radius. In order to analyze the correlation between building volume and change of wind speed, azimuth and radius was set, as shown in Table 2.

Fig. 10, 11, 12 shows Correlation Analysis of wind speed and building volume fraction at Gangnam, Yangcheon, and Pyungtaek, respectively. The building volume fraction has a negative correlation coefficient from -0.6 to -0.8 as the change of wind speed. This means wind speed is reduced with increasing building volume fraction. This confirms that the building of up-wind side causes a wind-speed decrease.

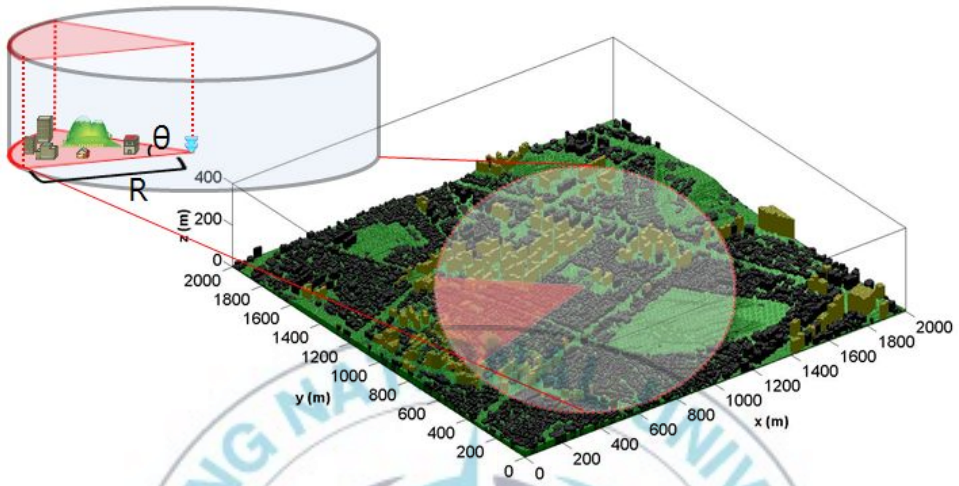


Fig. 9. Algorithm of building volume fraction calculation.

Table 2. The building volume fraction with consideration for R and  $\theta$ .

$\theta$ ( $^{\circ}$ ) \ R (m)	400	500	600	700
22.5	F <sub>1</sub>	F <sub>2</sub>	F <sub>3</sub>	F <sub>4</sub>
33.75	F <sub>5</sub>	F <sub>6</sub>	F <sub>7</sub>	F <sub>8</sub>
45	F <sub>9</sub>	F <sub>10</sub>	F <sub>11</sub>	F <sub>12</sub>

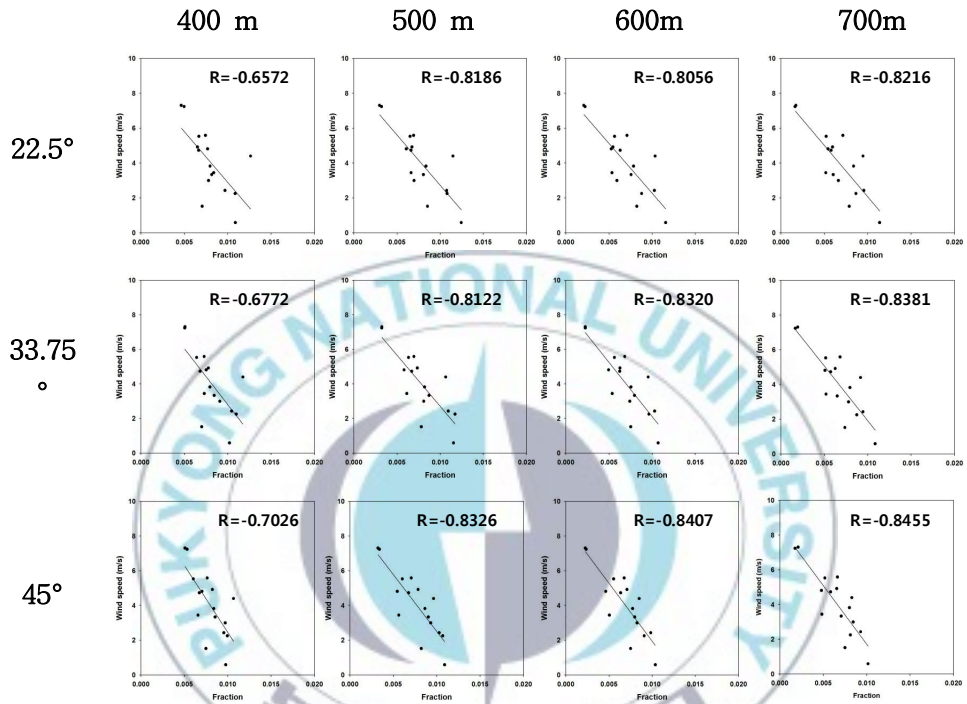
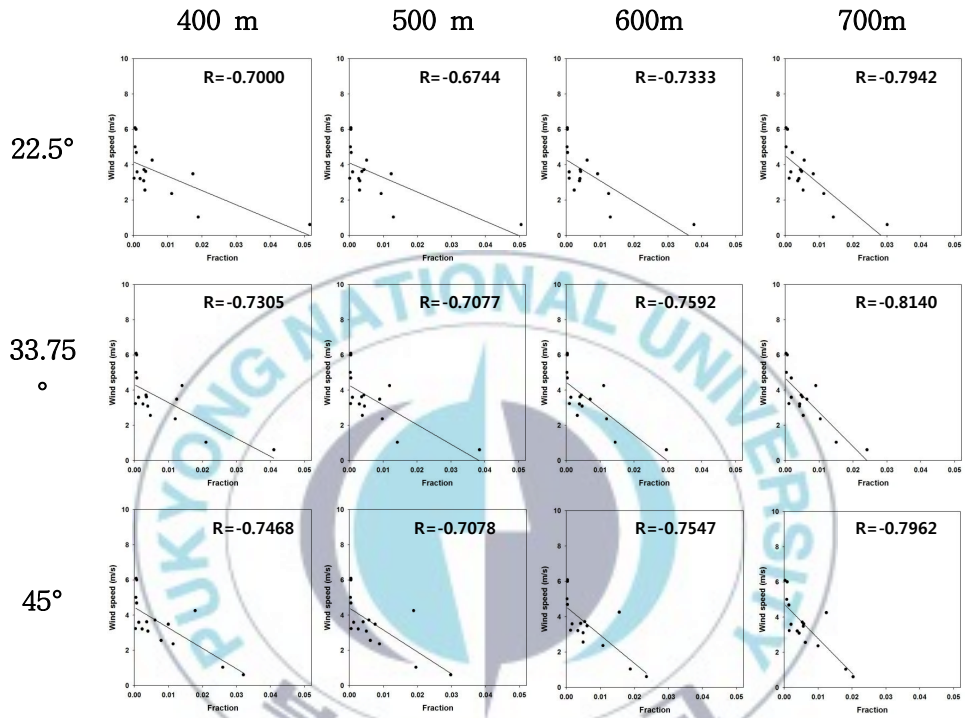
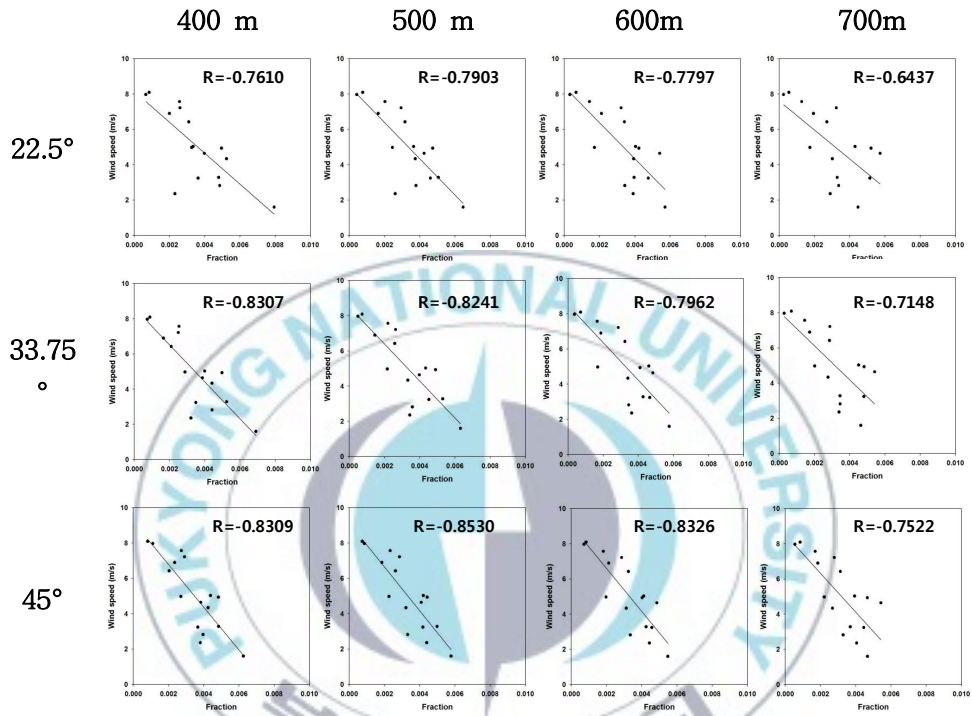


Fig. 10. Correlation Analysis of wind speed and building volume fraction at Gangnam.



**Fig. 11.** Correlation Analysis of wind speed and building volume fraction at Yangcheon.



**Fig., 12.** Correlation Analysis of wind speed and building volume fraction at Pyeongtaek.

### 3.4. Multiple regression analysis

Analysis of the correlation between building volume fraction and wind speed decreases confirms that the presence of up-wind side buildings plays a large role in wind-speed decreases. Also, increasing the building volume fraction on the up-wind side intensifies the decrease of wind speed at observation points. Therefore, the coefficient that can be used to correct the simulated wind speed by WRF model was developed using wind speed reduction with building volume fraction increasing.

Correction equation using developed coefficient is as eq. (7)

$$WS = \alpha \cdot WRF \quad (7)$$

Here, WS is corrected wind speed,  $\alpha$  is correction coefficient, WRF is simulated wind speed by WRF model

To calculate the correction coefficient that consider the factors as show in Table 2, Multiple regression analysis was used. Multiple regression analysis equation for calculation of correction coefficient is as eq. (8)

$$\alpha = b + \sum_{i=1}^n c_i F_i \quad (8)$$

Here,  $\alpha$  is correction coefficient,  $b$  is constant,  $c_i$  is regression constant of each independent variable, and  $F_i$  is building volume fraction.

The calculated correction coefficient of the 16 inflow directions is shown in Table 3.



**Table 3.** Correction coefficients of 16 wind directions at Target areas.

<b>Areas</b>	<b>Gangnam</b>	<b>Yangcheon</b>	<b>Pyeongtaek</b>
<b>N</b>	0.4170	0.5179	0.1652
<b>NNE</b>	0.4744	0.5519	0.4886
<b>NE</b>	0.6544	0.6662	0.3396
<b>ENE</b>	0.5410	0.6319	0.4987
<b>E</b>	0.3109	0.9451	0.7138
<b>ESE</b>	0.2477	0.9570	0.6551
<b>SE</b>	0.5513	0.6856	0.9598
<b>SSE</b>	1.0044	0.9039	1.1978
<b>S</b>	1.0295	0.6321	1.0872
<b>SSW</b>	0.8039	0.7319	0.9703
<b>SW</b>	0.7692	0.1004	0.6773
<b>WSW</b>	0.5927	0.1500	0.4315
<b>W</b>	0.5767	0.3840	0.9720
<b>WNW</b>	0.4309	0.4762	1.0791
<b>NW</b>	0.1958	0.5947	0.7089
<b>NNW</b>	0.3597	0.6342	0.7247

### 3.5. Validation

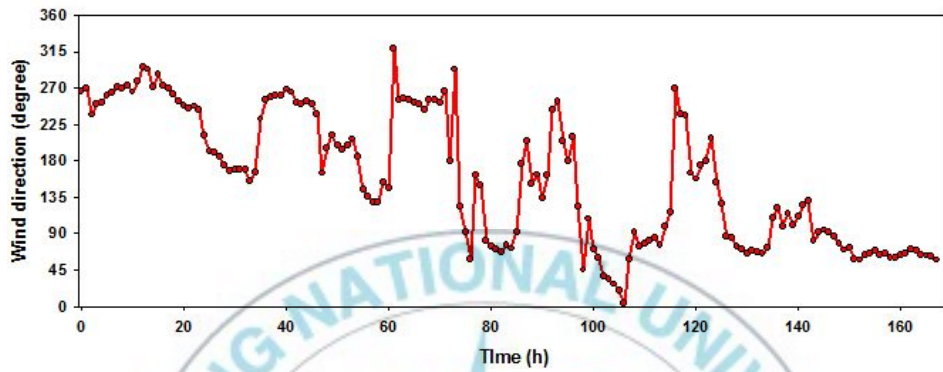
Simulated wind speeds from April 3rd to April 9th 2008 was corrected by correction coefficients at target areas.

Fig. 13 shows the wind direction of WFR simulation during the experiment period and the results of the wind speed correction at Gangnam areas. Overestimating the wind speed of WRF simulation was corrected using a correct coefficient. As a result, most of overestimated wind speed was close to observed wind speed. These results are analyzed by RMSE. The results of the RMSE showed that difference between the simulated wind speed and observed wind speed is  $3.17 \text{ ms}^{-1}$ . The RMSE corrected difference between the wind-speed and observed wind speed is  $1.53 \text{ ms}^{-1}$ . Corrected wind speed is closer than

The Yangcheon and Pyeongtaek areas are analyzed using the same methods. The results are shown in Fig. 14 and Fig. 15, respectively. In the case of Yangcheon and Pyungtaek areas, the RMSE between the simulated wind speed and observed wind speed is  $2.08 \text{ ms}^{-1}$  and  $2.80 \text{ ms}^{-1}$ , respectively. RMSE between the corrected wind speed and observed wind speed is  $1.32 \text{ ms}^{-1}$  and  $1.75 \text{ ms}^{-1}$ , respectively. The corrected wind speed is closer than the simulated wind in matching the observed wind-speed in all of target areas.

As a result, WRF simulation wind speed is close to the observed wind by using the correction coefficient using building volume fraction.

(a)



(b)

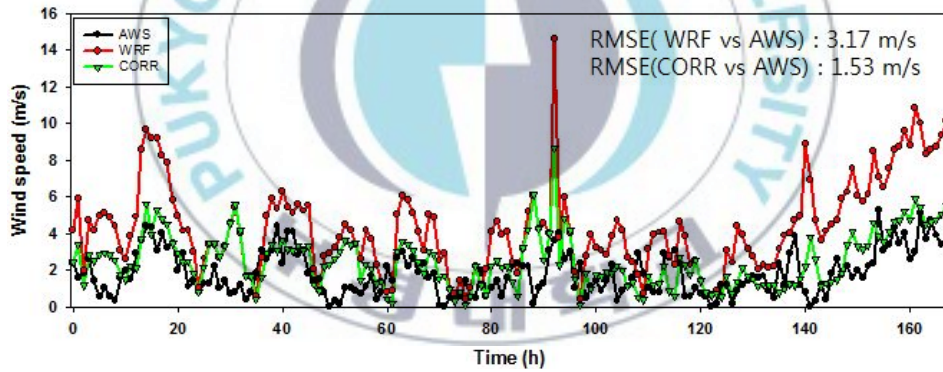
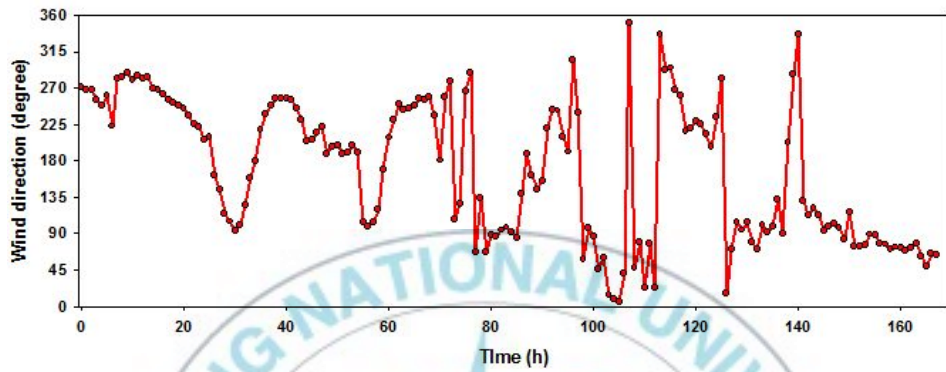


**Fig. 13.** (a) simulated wind direction of WRF model and (b) comparison of simulated wind speed of WRF model, observed wind speed, and corrected wind speed at Gangnam.

(a)



(b)

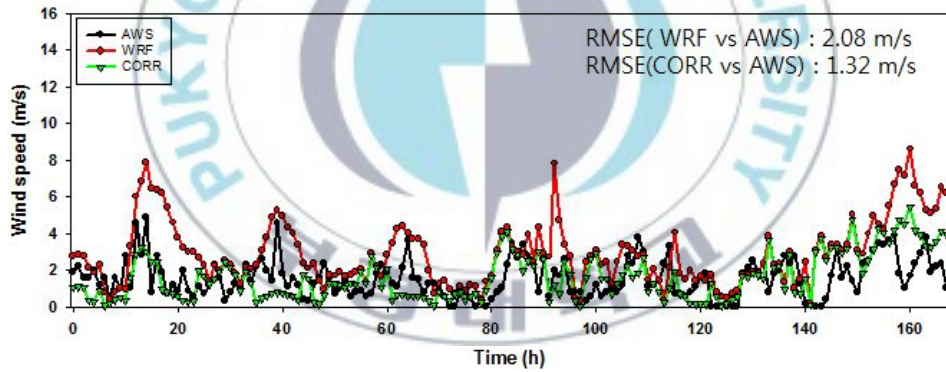
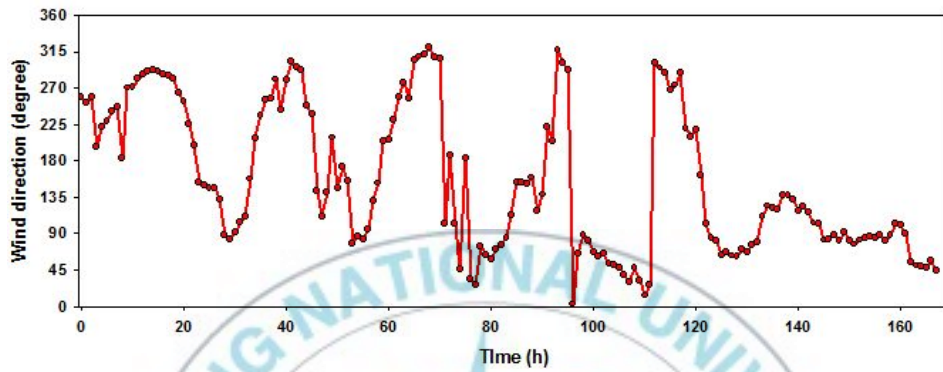


**Fig. 14.** (a) simulated wind direction of WRF model and (b) comparison of simulated wind speed of WRF model, observed wind speed, and corrected wind speed at Yangcheon.

(a)



(b)

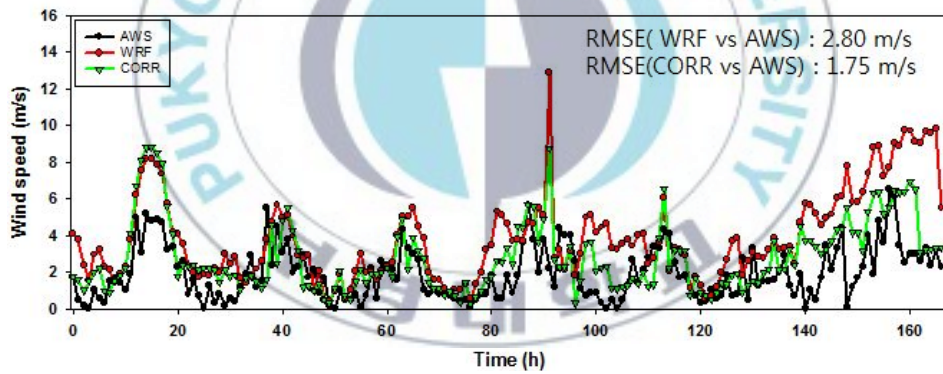


**Fig. 15.** (a) simulated wind direction of WRF model and (b) comparison of simulated wind speed of WRF model, observed wind speed, and corrected wind speed at Pyungtaek.

## 4. Summary and conclusions

In this study, for correction of simulated wind speed by WRF model, correction coefficient that can be reflect the effects of buildings in urban areas is developed using building volume fraction.

Simulated wind speed by WRF model and observed wind-speed are compared by observation stations in target areas(Gangnam, Yangcheon, and Pyeongtaek) that reflect the characteristics of the urban areas. The result of the comparison shows that the simulated wind-speed by WRF model tend to overestimates the results more than observational wind speed.

In order to determine the effects of structures in urban areas on change of wind speed, surface boundary input data that reflect the realistic terrain is created using GIS data. And Numerical simulation that consider the 16 case of inflow directions is carried out using CFD model. The result of the CFD simulation shows that the wind speed at observation point is decreased by fictional effects of surrounding buildings

In order to investigate the effects of building on change of wind speed, algorithm that calculate the building volume fraction on up-wind side is developed. Building volume fraction which is classified to 16 case of inflow directions is calculated using a developed algorithm.

Correlation between building volume fraction and wind speed is investigated at target areas. As a result, Correlation between building volume fraction and wind speed appears that negative correlation coefficient from -0.6 to -0.8

In order to product the corrected wind speed that reflect the building effects in urban areas, correction coefficient is calculated by multiple regression analysis using a result of CFD simulation and building volume fraction.

Simulated wind speed by WRF model was corrected by the each correction coefficients of target areas. As a result, WRF simulation wind speed is close to the observed wind by the correction coefficient.

Developed method using correction coefficient can be improve the error of WRF simulation wind speed by frictional effects of the building. WRF users can be produce the more accurate wind speed information in urban areas with out CFD model simulation through construction of wind speed correction coefficient data base for major urban areas. Also, developed method can be provide the base of urban parameterization

Finally, in this study, the correct of the simulated wind speed is carried out using building volume fraction. But correction of wind speed and analyze using various factor are necessary. Also, followup study for improvement of correct of the simulated wind speed is needed.

## 5. Reference

- 김재진, 백종진, 2005: CFD 모형을 이용한 도시 지역 흐름 및 스칼라 분산 연구. 한국기상학회지, 41, 821-837.
- 이영수, 김재진, 2011: 도시 지역에서 아파트 단지가 흐름과 확산에 미치는 영향. 대기, 21, 95-108.
- 이화운, 정우식, 김현구, 이순환, 2003: 대기오염 확산 해석을 위한 포항지역 기상장 연구. 한국대기환경학회지, 20, 1-15.
- 최민규, 여현구, 천만영, 선우영, 2002: 도시 대기 중 유기염소계 살충제의 농도수준 및 배출 특성, 한국대기환경학회지, 18, 275-284.
- Baik, J.-J., and J.-J. Kim, 1999: A numerical study of flow and pollutant dispersion characteristics in urban street canyons. *J. Appl. Meteor.*, 38, 1576-1589.
- , J.-J. Kim, and H. J. S. Fernando, 2003: A CFD model for simulating urban flow and dispersion. *J. Appl. Meteor.*, 42, 1636-1648.
- , R.-S. Park, H.-Y. Chun, and J.-J. Kim, 2000: A laboratory model of urban street-canyon flows. *J. Appl. Meteor.*, 39, 1592-1600.
- Brown, M. J., R. E. Lawson Jr., D. S. DeCroix, and R. L. Lee, 2000: Mean flow and turbulence measurements around a 2-D array of buildings in a wind tunnel. 11th Joint Conference on the Applications of Air Pollution Meteorology with the A&WMA, Long Beach, CA, USA, 35-40.
- Cheng, X., and F. Hu, 2005: Numerical studies on flow fields around buildings in an urban street canyon and cross-road. *Adv. Atmos. Sci.*, 22, 290-299.

- DePaul, F. T., and C. M. Sheih, 1986: Measurements of wind velocities in a street canyon. *Atmos. Environ.*, 20, 455-459.
- Dudhia, J., 1996: A multi-layer soil temperature model for MM5. 6th Annual PSU/NCAR MesoscaleModel (MM5 )Users Workshop, Penn. State Univ., Boulder ,CO., USA.
- Hong, S.-Y., and J.-O. J. Lim, 2006: The WRF single-moment 6-class microphysics scheme (WSM6). *J. Korean Meteor. Soc.*, 42, 129-151.
- Janjić, Z. I., 2001: Nonsingular implementation of the Mellor-Yamada level 2.5 scheme in the NCEP meso model. National Centers for Environmental Prediction, Office Note #437, 61 pp.
- Kain, J. S., and J. M. Fritsch, 1993: Convective parameterization for mesoscale models: The Kain-Fritsch scheme, The representation of cumulus convection in numerical models. edited by K. A. Emanuel and D. J. Raymond, *Am. Meteorol. Soc.*, Boston, MA., USA, 246 pp.
- Kim, J.-J., and J.-J. Baik, 1999: A numerical study of thermal effects on flow and pollutant dispersion in urban street canyons. *J. Appl. Meteor.*, 38,1249-1261.
- \_\_\_\_\_, and \_\_\_\_\_, 2001: Urban street-canyon flows with bottom heating. *Atmos. Environ.*, 35, 3395-3404.
- \_\_\_\_\_, and \_\_\_\_\_, 2005: Physical experiments to investigate the effects of street bottom heating and inflow turbulence on urban street-canyon flow. *Adv. Atmos .Sci.*, 22, 230-237.
- Lee, I. Y., and H. M. Park, 1994: Parameterization of the pollutant transport and dispersion in urban street canyons. *Atmos. Environ.*, 28, 2343-2349.
- Liu, C.-H., and M. C. Barth, 2002: Large-eddy simulation of flow and scalar transport in a modeled street canyon. *J. Appl. Meteor.*, 41, 660-673.

- Liu, H. Z., B. Liang, F. R. Zhu, B. Y. Zhang, and J. G. Sang, 2003: A laboratory model for the flow in urban street canyons induced by bottom heating. *Adv. Atmos.Sci.*, 20, 554-564.
- Mitchell, K., 2005: The community Noah Land-Surface Model (LSM). [Available online at [ftp://ftp.emc.ncep.noaa.gov/mmb/gcp/ldas/noahlsn/ver\\_2.7.1](ftp://ftp.emc.ncep.noaa.gov/mmb/gcp/ldas/noahlsn/ver_2.7.1)]
- Nakamura, Y., and T. R. Oke, 1988: Wind, temperature, and stability conditions in an east-west oriented urban canyon. *Atmos.Environ.*, 22, 2691-2700.
- Otte, Tanya L., A. Lacser, S. Dupont, J. K. S. Ching, 2003: Implementation of an Urban Canopy Parameterization in a Mesoscale Meteorological Model. *J. Appl. Meteor.*, 43, 1648-1664.
- Patankar, S. V., 1980: *Numerical Heat Transfer and Fluid Flow*. McGraw-Hill, New York, 197 pp.
- Rotach, M. W., 1995: Profiles of turbulence statistics in and above an urban street canyon. *Atmos. Environ.*, 29, 1473-1486.
- Sini, J.-F., S. Anquetin, and P. G. Mestayer, 1996: Pollutant dispersion and thermal effects in urban street canyons. *Atmos. Environ.*, 30, 2659-2677.
- Uehara, K., S. Murakami, S. Oikawa, and S. Wakamatsu, 2000: Wind tunnel experiments on how thermal stratification affects flow in and above urban street canyons. *Atmos. Environ.*, 34,1553-1562.
- United Nations, Department of Economic and Social Affairs, Population Division, 2012: *World urbanization Prospects: The 2011 Revision, File1: Population of Urban and Rural Areas and Percentage Urban, 2011*
- Versteeg, H. K., and W. Malalasekera, 1995: *An Introduction to*

Computational Fluid Dynamics: The Finite Volume Method.  
Longman, Malaysia, 257 pp.

Yakhot, V., S. A. Orszag, S. Thangam, T. B. Gatski, and C. G. Speziale, 1992: Development of turbulence models for shear flow by a double expansion technique. *Physics of Fluids*, 4, 1510-1520.

